CAV2021
11th International Symposium on Cavitation
May 10-13, 2021, Daejeon, Korea

Development of generalized CFD model for cavitating flows

Sachin Zanje[1], Kannan Iyer[2], Janani Srree Murallidharan[1], Hemant Punekar[3], Padmesh Mandloi[3], Vinay Kumar Gupta[3]

[1]Department of Mechanical Engineering, IIT Bombay, Mumbai-400076, India
[2]Department of Mechanical Engineering, IIT Jammu, Jammu-181221, India
[3]ANSYS Software Pvt. Ltd., 34/1 Rajiv Gandhi Infotech Park, Pune-411057, India

Abstract: Cavitation occurs in a wide range of applications such as marine propellers, diesel injectors, supercavitating projectiles, etc. Currently available cavitation models have empiricism built into it through the various constants used along with the Rayleigh's expression for bubble growth and collapse in rate of evaporation and condensation respectively. Rayleigh's expression is based on only the inertial growth and collapse of vapour bubble. However, there are many applications such as cavitation in control valve of a boiler, cryogenic cavitation etc., where thermal effects dominate. Therefore to develop a generalized cavitation model, it is necessary to consider thermal effects in addition to the hydrodynamic effects on bubble growth and collapse rates. In the present work the generalized expression developed for growth over a wide range of Jakob number is utilized. The collapse rate is approximated by considering symmetry with the bubble growth rate expression. The model developed is benchmarked for cavitation around hemispherical head projectile for water and cryogenic cavitation around a hydrofoil for liquid nitrogen. The newly developed generalized cavitation model shows better agreement with the experimental data for both water and cryogenic cavitation.

Keywords: Inertia; thermal; bubble growth; cavitation; cryogenic.

1. Introduction

Cavitation occurs in wide range of applications such as isothermal cavitation where inertia effects are dominating or cryogenic cavitation where thermal effects are dominating. Presently available cavitation models [1-4] account only for the inertial bubble growth regime [5] which leads to deviations in the evaporation rate when thermal effects dominate. Therefore there is a need for a general cavitation model that accounts for both inertia as well as thermal effects. In the present work, a mechanistic model is developed for bubble growth rate expression from one dimensional solution of complete Rayleigh-Plesset equation to account for thermal as well as hydrodynamic regimes of bubble growth.

2. Cavitation modelling

Homogeneous mixture model with implicit formulation is used to simulate the physical phenomena of cavitation. The mixture model solves the continuity and momentum equation for a mixture and the volume fraction equation for vapour. The SST k-ω model is used to account for the effect of turbulence on

* Corresponding Author: Sachin Zanje, sachin.zanje@iitb.ac.in

cavitation. The source and sink terms for the vapour transport equation are generated from Schnerr and Sauer [2] model as,

If $P \leq P_v$, the evaporation expression gets triggered:

$$\dot{m}_e = C_{evap} \frac{\rho_l \rho_v}{\rho} \alpha(1-\alpha) \frac{3}{R} \frac{dR}{dt} \tag{1}$$

If $P \geq P_v$, the condensation expression gets triggered:

$$\dot{m}_c = C_{cond} \frac{\rho_l \rho_v}{\rho} \alpha(1-\alpha) \frac{3}{R} \frac{dR}{dt} \tag{2}$$

In Schnerr and Sauer [2] model, growth and collapse rate expressions are used from Rayleigh [5] as,

$$\frac{dR}{dt} = \pm\sqrt{\frac{2}{3}\left(\frac{P_v - P}{\rho_l}\right)} \tag{3}$$

The evaporation coefficient (C_{evap}) used in the present work is 1. The bubble growth rate expression dR/dt is related to nondimensionalized quantities R^+ and t^+ as,

$$\frac{dR}{dt} = A\frac{dR^+}{dt^+} \tag{4}$$

Where, radius and time are nondimensionalized similar to [6] as,

$$\left.\begin{aligned} R^+ = \frac{AR}{B^2} \; and \; t^+ = \frac{A^2 t}{B^2} \\ A = \left(\frac{2}{3}\frac{\rho_v h_{fg}(T_\infty - T_{sat})}{\rho_l T_{sat}}\right)^{\frac{1}{2}}, B = \left(\frac{12}{\pi} a_l\right)^{\frac{1}{2}} J_a \; and \; J_a = \frac{\rho_l Cp_l (T_\infty - T_{sat})}{\rho_v h_{fg}} \end{aligned}\right\} \tag{5}$$

In Eq. (5) liquid properties (a_l, Cp_l, ρ_l) are obtained at local temperature (T_∞) and ρ_v, h_{fg}, T_{sat} are obtained as saturation properties at local pressure (P). The one dimensional numerical model developed by [7] for bubble growth. Based on this model, parametric studies are carried out for obtaining non-dimensional bubble growth rate (Eq. (6)) and the results generated are presented in the form of a generalized correlation [7]. This asymptotic nondimensional bubble growth rate (Eq. (6)) considers both thermal and inertial effects. It was derived for Jakob number range of $6.36 < J_a < 2745$.

$$\frac{dR^+}{dt^+} = 1.172[(1+t^+)^{0.4586} - (t^+)^{0.4586}] \tag{6}$$

Although this expression is similar to the one obtained by [6], which uses an analytical method. Authors in [7] obtained different coefficients using numerical approach. To utilize Eq. (6) there was a need to track each individual bubble from inception to final growth, due to presence of bubble growth time in the expression, which becomes computationally costly. Therefore in present work the time is transformed into appropriate spatial dimension, which is applicable for both steady and unsteady flow problems. Based on this transformation the growth rate is computed (Eq. (4)). More details about this transformation are not published here owing to confidential agreement with the project sponsors. For bubble collapse, the rate of collapse is assumed to follow the same trend as that of the growth curve except in the reverse direction. However, upon investigation, we found that collapse rates predicted by our model are significantly lower than growth rates, and hence an additional condensation coefficient (C_{cond}) = 0.1 is included to compensate for the deviation. The evaporation and condensation rates based on Eq. (3) and (4) are implemented in ANSYS Fluent through user defined functions.

3. Results

3.1. Cavitation around hemispherical head projectile

The first benchmark problem taken for comparing the cavitation models is flow around hemispherical head projectile with the critical Reynolds number of 2×10^5. From experimental data of [8], the diameter (d) of hemispherical head and cylindrical shank is 25.4 mm. The properties of liquid are calculated by

* Corresponding Author: Sachin Zanje, sachin.zanje@iitb.ac.in

assuming water at 30℃. Based on critical Reynolds number and properties of water at 30℃ the free stream velocity (U_∞) over hemispherical head body is 6.3 m/s. In the present work the numerical results are compared with experimental data at cavitation number $\sigma = 0.3$. The hemispherical forebody and cylindrical shank projectile has diameter d = 25.4 mm and domain length of 12d is considered since pressure distribution over cylindrical surface is almost settling to outlet pressure at s/d = 6 from experimental data of [8], where s is the distance along the surface of body. This projectile is kept in water tunnel of square cross-section $304.8 \times 304.8\ mm^2$, therefore domain height is considered as 6d. As the flow conditions need to be uniform till the cylinder the upstream length of domain from stagnation point is taken as 5d. Based on the above specifications, the details of computational domain are shown in Figure 1.

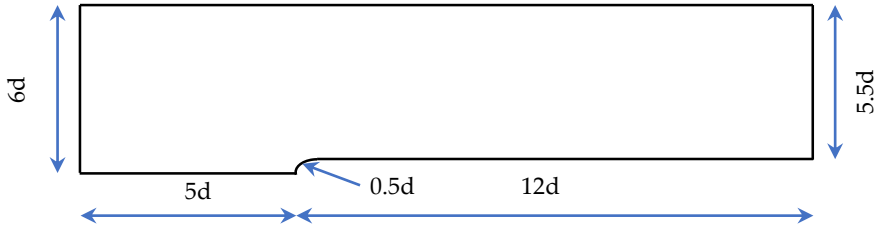

Figure 1. Computational domain for hemispherical forebody projectile

The structured grid for 2D axisymmetric domain is created in ICEM CFD. The grid sensitivity is done for number of cells of 14196, 31152, 54826 and 85140. The pressure distribution is insensitive when mesh size is finer than 54826. Therefore grid size of 54826 is optimum for simulations. The simulations are done by using homogeneous mixture model for water and vapour with constant properties. Pressure based coupled solver with Pseudo-transient time formulation is used with SST $k-\omega$ model for turbulence. The results obtained from generalized cavitation model using bubble number density of 1×10^9 is compared with experimental data of [8] at cavitation number of 0.3 for pressure coefficient (C_p) along the projectile surface. The results show good agreement with the experimental data as shown in Figure 2. Schnerr and Sauer [2] model using bubble number density of 1×10^9 also is in good agreement with the experimental data.

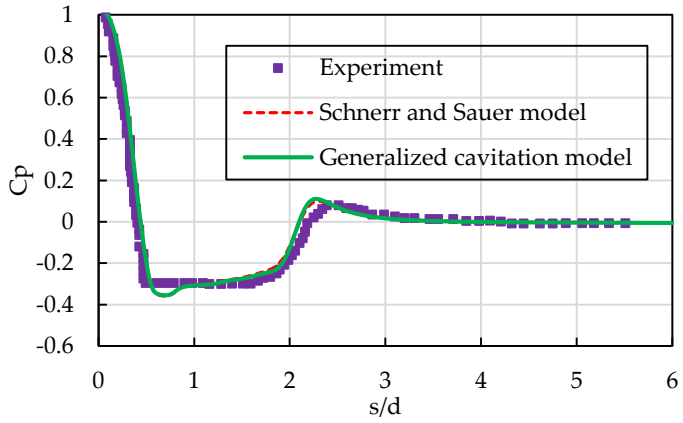

Figure 2. Comparison of pressure variation with experimental data of [8] at $\sigma = 0.3$

3.2. Cryogenic cavitation around hydrofoil

* Corresponding Author: Sachin Zanje, sachin.zanje@iitb.ac.in

The second benchmark problem is identified as flow of liquid nitrogen around a hydrofoil. In the experiment of [9] hollow hydrofoil is kept in a square channel of size $25.4 \times 25.4\ mm^2$ with the help of a mandrel. The chord length of hydrofoil is 63.5 mm and the hydrofoil consists of cylindrical head of radius 3.96 mm. Based on these specifications the computational domain is identified and the details of computational domain for hydrofoil considered from [9] are as shown in Figure 3.

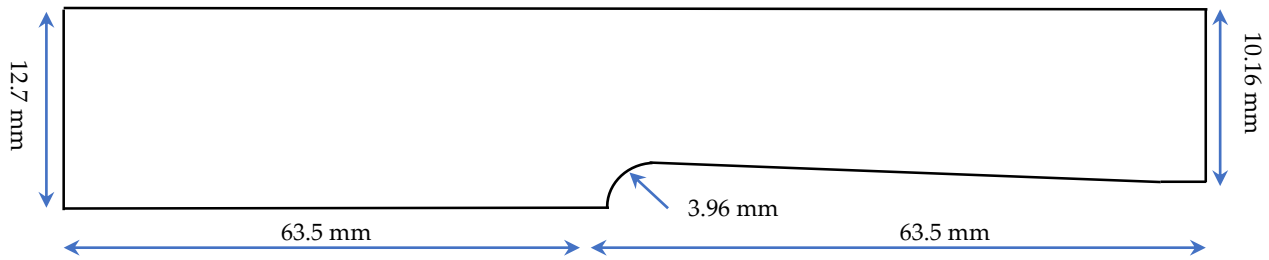

Figure 3. Computational domain for hydrofoil

This benchmark is chosen to check the applicability of generalized cavitation model to account for thermal effect without solving the energy equation. In this work we have done comparisons for the generalized cavitation model for 290C and 296B cases for liquid nitrogen at bubble number density of 1×10^{12}. To check the applicability of Schnerr and Sauer model [2] for cryogenic cavitation the results are compared for model under isothermal conditions at bubble number density of 1×10^{11}. The operating conditions for these two cases of liquid nitrogen are shown in Table 1.

Table 1. Operating conditions for cryogenic case [9]

Case	T_∞ (K)	U_∞ (m/s)	σ	R_e
290C	83.06	23.9	1.7	9.93×10^6
296B	88.54	23.7	1.61	1.11×10^7

The results from 2D simulations for pressure depression ($P-P_v$) along hydrofoil surface for 290C and 296B with velocity inlet (U_∞) and pressure outlet boundary condition are compared as shown in Figures 4 (a) and 4 (b) respectively. The numerical setup is similar to hemispherical head case as discussed in Section 3.1 for computational grid with 82683 elements. The generalized cavitation model shows better agreement with experimental data of [9] in comparison with Schnerr and Sauer [2] model. This deviation in Schnerr and Sauer model is mainly because of neglecting the thermal term in the Rayleigh-Plesset equation. The thermodynamic parameter [10] is used to assess the thermodynamic effect in cavitating flows. For cryogenic cases this parameter is of more importance [11], which is neglected in the isothermal Schnerr and Sauer model. To account for thermal effects in Schnerr and Sauer model we also solved energy equation along with the Rayleigh's expression (Eq. (3)) with vapour pressure (P_v) and thermo physical properties ($\rho_l, \rho_v, Cp_l, Cp_v$) as function of temperature. The results shown in Figure 4 with energy equation for Schnerr and Sauer model. The generalized cavitation model gives very good agreement with experimental data even without solving energy equation because of thermal term consideration and property variations with local pressure which is already built in into the bubble growth rate expression (Eq. (6)).

* Corresponding Author: Sachin Zanje, sachin.zanje@iitb.ac.in

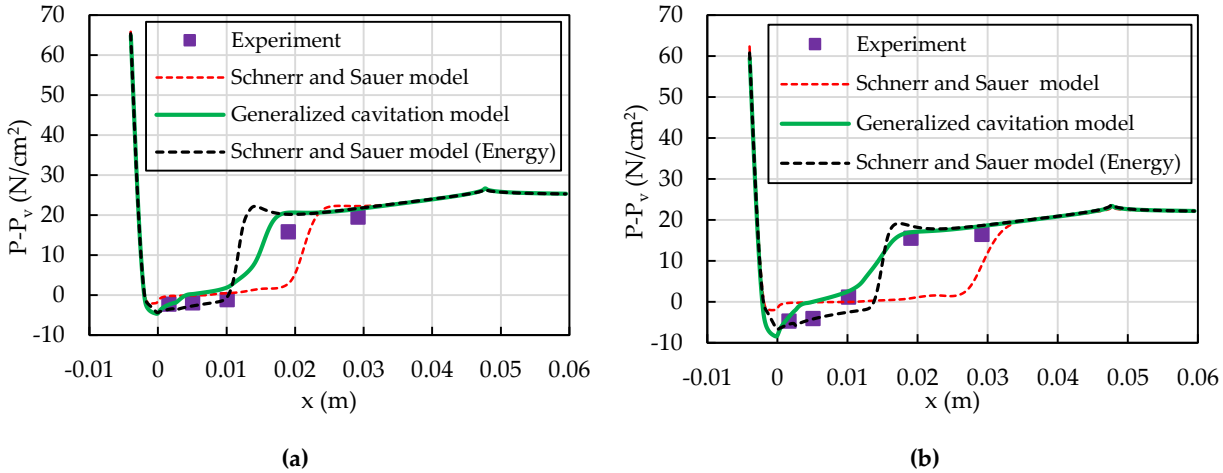

Figure 4. Comparison of pressure depression with experimental data of [9] on hydrofoil surface for (a) 290C (b) 296B

4. Conclusions

A generalized cavitation model is developed based on bubble dynamics of single bubble using an expression that accounts for inertia as well as thermal effects. The validations show a good agreement with experiments with water and liquid nitrogen.

Acknowledgments: This work is financially supported by ANSYS Software Pvt. Ltd., Pune, India.

References

1. Kubota, A.; Kato, H. and Yamaguchi, H. A new modelling of cavitating flows: a numerical study of unsteady cavitation on a hydrofoil section. *Journal of Fluid Mechanics* 1992, *240*, pp. 59-96.
2. Schnerr, G. H. and Sauer, J. Physical and numerical modeling of unsteady cavitation dynamics. *Fourth International Conference on Multiphase Flow* 2001, pp. 1–12.
3. Singhal, A.K.; Athavale, M.M.; Li, H. and Jiang, Y. Mathematical basis and validation of the full cavitation model. *Journal of Fluids Engineering*, 2002, *124(3),* pp. 617-624.
4. Zwart, P.J.; Gerber, A.G. and Belamri, T. A two-phase flow model for predicting cavitation dynamics. *International Conference on Multiphase Flow* 2004, *152*.
5. Rayleigh, L. VIII. On the pressure developed in a liquid during the collapse of a spherical cavity. *The London, Edinburgh, and Dublin Philosophical Magazine and Journal of Science* 1917, *34(200),* pp. 94-98.
6. Mikic, B.B.; Rohsenow, W.M. and Griffith, P. On bubble growth rates. *International Journal of Heat and Mass Transfer* 1970, *13(4),* pp. 657-666.
7. S. Zanje, K. Iyer, J. S. Murallidharan, H. Punekar and V. K. Gupta. Development of generalized bubble growth model for boiling and cavitation. *International Journal of Multiphase flow* (under review).
8. Rouse, H. and McNown, J.S. Cavitation and pressure distribution: head forms at zero angle of yaw. Iowa Institute of Hydraulic Research, Iowa, 1948.
9. Hord, J. Cavitation in liquid cryogens. 2: Hydrofoil, National Aeronautics and Space Administration, Washington, 1973.
10. Brennen, C. E. *Cavitation and Bubble Dynamics*. Oxford University Press, Oxford, 1995; pp. 30-58.
11. Chen, T.; Huang, B.; Wang, G. and Wang, K. Effects of fluid thermophysical properties on cavitating flows. *Journal of Mechanical Science and Technology* 2015, 29(10), pp. 4239-46.

* Corresponding Author: Sachin Zanje, sachin.zanje@iitb.ac.in